2011

Incremental Binding Energies of Gold (I) and Silver (I) Thiolate Clusters

Brian M. Barngrover
Stephen F Austin State University, barngrovbm@sfasu.edu

Christine M. Aikens

THE JOURNAL OF PHYSICAL CHEMISTRY A

ARTICLE

pubs.acs.org/JPCA

Incremental Binding Energies of Gold(I) and Silver(I) Thiolate Clusters

Brian M. Barngrover and Christine M. Aikens*

Department of Chemistry, Kansas State University, Manhattan, Kansas 66506, United States

ABSTRACT: Density functional theory is used to find incremental fragmentation energy, overall dissociation energy, and average monomer fragmentation energy of cyclic gold(I) thiolate clusters and anionic chain structures of gold(I) and silver(I) thiolate clusters as a measure of the relative stability of these systems. Two different functionals, BP86 and PBE, and two different basis sets, TZP and QZ4P, are employed. Anionic chains are examined with various residue groups including hydrogen, methyl, and phenyl. Hydrogen and methyl are shown to have approximately the same binding energy, which is higher than phenyl. Gold−thiolate clusters are bound more strongly than corresponding silver clusters. Lastly, binding energies are also calculated for pure $Au_{25}(SR)_{18}^-$, $Ag_{25}(SR)_{18}^-$, and mixed $Au_{13}(Ag_2(SH)_3)_6^-$ and $Ag_{13}(Au_2(SH)_3)_6^-$ nanoparticles.

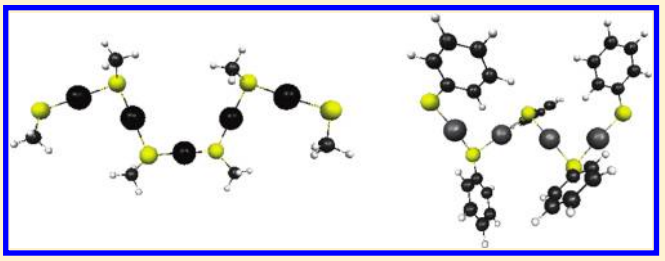

INTRODUCTION

The precious metals of gold and silver have held special value to us since their discovery. Historically they were used as currency; now, however, they are used in many more applications, especially when employed on the nanoscale level with ligands. Some of the applications for gold(I) thiolate clusters are in antiarthritic and antitumor drugs as well as protein labeling, drug delivery, and sensing.[1−3] Silver thiolate clusters have applications as biosensors.[4]

In 2006, two groups independently studied the structures for cyclic metal methylthiolate clusters using density functional theory (DFT) and found essentially the same lowest energy configurations.[5,6] Howell investigated $M_n(SR)_n$ (M = Cu, Ag, Au and n = 2−6) rings and found that the strain on the system is relieved at n = 4.[5] Grönbeck et al. studied the structures and fragmentation energies of cyclic $(AuSR)_n$ (R = CH_3, n = 2−12) using PBE.[6] They found that the smallest systems had planar structures while the larger structures went to a crown-like zigzag configuration.[6] The fragmentation energies of the systems converged at n = 4.[6] They showed that larger ligands such as hexylthiolate, benzenthiolate, and glutathionate have minor differences on the Au−S framework structure but negligible effects on the highest occupied molecular orbital to lowest unoccupied molecular orbital (HOMO−LUMO) gap.[6]

More recent work by Zeng and co-workers suggested helical and catenane structures for the larger systems (n = 6−12).[7] A later study by Kacprzak et al. agreed that catenane structures are preferred for n = 10−12 but found crown structures to be lower energy than helical structures for n = 6−9.[8] They also examined fragmentation energy as a function of the metal and found Cu > Au > Ag.[8]

Experimentally, gold(I) complexes have been crystallized and observed by many different groups.[2,9−11] The gold(I) crystals seen by Bau are helical in nature.[2] Simpson et al., LeBlanc and co-workers, and Wiseman et al. have all observed cyclic ring structures of gold(I) complexes.[9−11] Wiseman et al. also observed catenane structures for larger gold(I) clusters (n = 10, 12).[11]

Silver(I) complex crystals have also been synthesized and characterized by many groups.[12−16] Ahmed and co-workers have performed X-ray crystallography and observed tetrameric ring structure for a large silver(I) complex, whereas smaller structures adopt a chairlike configuration.[12] Dance et al. have studied many different silver(I) complexes by using X-ray crystallography and NMR and have seen cyclic clusters, bridged-linked monocyclic clusters, and layered silver(I) clusters.[13−16]

In addition, anionic chains such as $Au(SR)_2^-$ and $Au_2(SR)_3^-$ are observed on the outside of the core of many different size nanoparticles such as $Au_{25}(SR)_{18}^-$, $Au_{38}(SR)_{24}$, and $Au_{102}(SR)_{44}$.[17−22] They have been predicted to passivate $Au_{144}(SR)_{60}$[23] and are observed on self-assembled monolayers (SAMs).[24−27] A longer $Au_3(SR)_4^-$ chain was predicted by Zeng et al. and by Jiang et al. to passivate $Au_{20}(SR)_{16}$.[28,29] Moreover, these motifs could be precursors in nanoparticle growth.[30] In this work we calculate the binding energies of anionic chains since these could affect the sizes and structures of nanoparticles. The electronic structure and optical absorption of pure $Au_{25}(SH)_{18}^-$, $Ag_{25}(SH)_{18}^-$, and mixed $Au_{13}(Ag_2(SH)_3)_6^-$ and $Ag_{13}(Au_2(SH)_3)_6^-$ systems have previously been studied by Aikens,[31] so binding energies of the $M_2(SR)_3^-$ chains to the 13-atom icosahedral cores are also studied in this work.

COMPUTATIONAL METHODS

The fragmentation energies for the gold and silver clusters are determined by using DFT with Becke Perdew (BP86)[32,33] and Perdew−Burke−Ernzerhof (PBE)[34] functionals and polarized triple-ζ (TZP) and quadruple-ζ (QZ4P) basis sets. A few

Received: June 30, 2011
Revised: September 7, 2011
Published: September 26, 2011

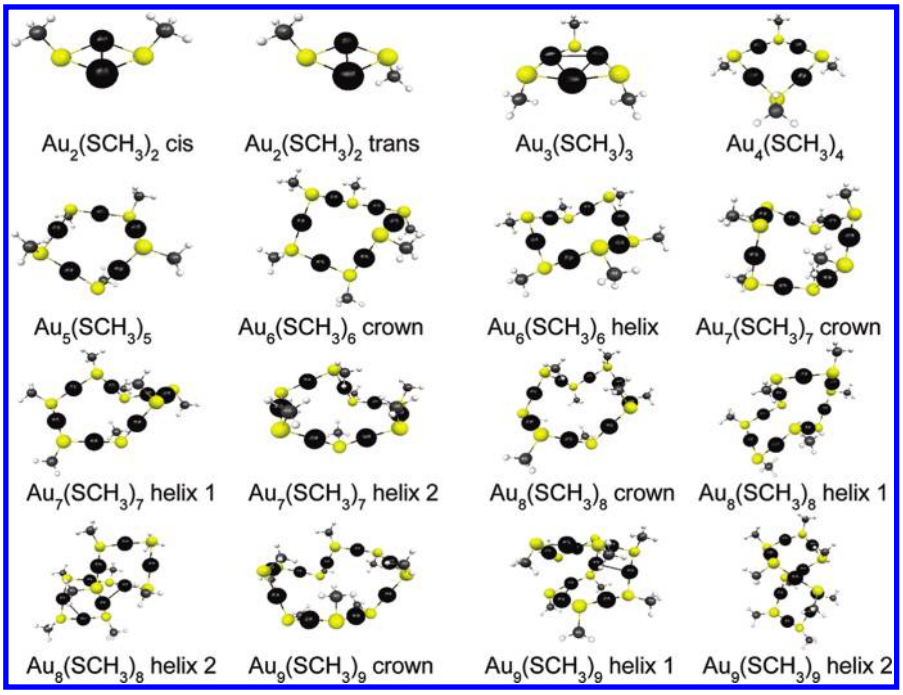

Figure 1. Optimized cyclic structures for $Au_x(SCH_3)_x$ (x = 2−9). Key: Au: black; S: yellow; C: gray; H: white.

Table 1. Binding Energies of Cyclic Gold Methylthiolate Clusters

	BP86/TZP			PBE/TZP			PBE (ref 6)	
group size	E_{inc} (eV)	E_{av} (eV)	E_{total} (eV)	E_{inc} (eV)	E_{av} (eV)	E_{total} (eV)	E_{inc} (eV)	E_{av} (eV)
dimer cis	1.07	0.54	21.59	1.17	0.58	21.69	1.16	0.58
dimer trans	1.09	0.55	21.61	1.18	0.59	21.70		
trimer	4.00	1.69	35.86	4.07	1.75	36.04	4.07	1.74
tetramer	2.58	1.91	48.69	2.65	1.98	48.95	2.61[a]	1.96
pentamer	1.95	1.92	60.91	2.02	1.99	61.23	1.97	1.97
hexamer-crown	1.89	1.92	73.06	1.96	1.98	73.45	2.01	1.98
hexamer-helix	1.89	1.92	73.06	2.05	2.00	73.55		
heptamer-helix 1	1.95	1.92	85.27	2.03	2.00	85.84		
heptamer-helix 2	1.96	1.92	85.27	2.00	2.00	85.80		
heptamer-crown	1.93	1.92	85.25	2.08	2.00	85.79	1.96	1.98
octomer-helix 1	1.93	1.92	97.46	1.99	2.00	98.09		
octomer-helix 2	1.91	1.92	97.45	2.05	2.00	98.11		
octomer-crown	2.01	1.93	97.52	2.03	2.00	98.08	2.01	1.98
nonomer-helix 1	1.83	1.91	109.55	1.99	2.00	110.35		
nonomer-helix 2	1.95	1.92	109.66	2.05	2.01	110.43		
nonomer-crown	1.89	1.93	109.68	1.97	2.00	110.31	1.96	1.97

[a] Corrected value (originally reported as 1.96).

energies have also been calculated with the Tao−Perdew−Staroverov−Scuseria (TPSS) functional.[35] All calculations are performed using the Amsterdam Density Functional (ADF)[36] package. We include scalar relativistic effects by incorporating zero order regular approximation (ZORA).[37] The cluster sizes range from one to four metal atoms with corresponding thiolate ligands, which have hydrogen, methyl, or phenyl groups. Both functionals were also used to find the fragmentation energies of the cyclic gold thiolate clusters ranging from two to nine metal atoms.[6−8] Energies for both functionals are compared. The energies of interest are the incremental fragmentation energy, calculated as $E_{inc} = E[RS(MSR)_n^-] - E[MSR] - E[RS(MSR)_{n-1}^-]$ (M = Au, Ag and R = H, CH_3, Ph), and the overall dissociation energy, which is calculated as $E_{total} = E[RS(MSR)_n^-] - (n+1)E[SR^-] - nE[M^+]$. In addition, an average monomer fragmentation energy is computed for cyclic systems as $E_{av} = [E[(AuSR)_n] - nE[AuSR]]/n$. The incremental and overall dissociation energies for the gold and silver clusters are calculated to determine the stability of the clusters. The same calculations are done on the mixed metal core nanoparticles for

Table 2. Binding Energies of Gold- and Silver-Thiolate Anionic Chains

	BP86/TZP		PBE/TZP	
	E_{inc} (eV)	E_{total} (eV)	E_{inc} (eV)	E_{total} (eV)
$Au(SH)_2^-$	3.24	13.21	3.30	13.30
$Au_2(SH)_3^-$	2.40	25.59	2.46	25.75
$Au_3(SH)_4^-$	2.14	37.70	2.18	37.93
$Au_4(SH)_5^-$	2.03	49.70	2.07	49.99
$Au_5(SH)_6^-$	2.00	61.68	2.08	62.07
$Au(SCH_3)_2^-$	3.22	13.48	3.29	13.57
$Au_2(SCH_3)_3^-$	2.32	26.07	2.36	26.20
$Au_3(SCH_3)_4^-$	2.13	38.46	2.23	38.70
$Au_4(SCH_3)_5^-$	2.02	50.74	2.09	51.06
$Au_5(SCH_3)_6^-$	2.01	63.01	2.10	63.43
$Au(SPh)_2^-$	2.99	12.45	3.01	12.40
$Au_2(SPh)_3^-$	2.15	23.97	2.15	23.94
$Au_3(SPh)_4^-$	1.94	35.36	2.07	35.40
$Au_4(SPh)_5^-$	1.83	46.64	1.99	46.78
$Ag(SH)_2^-$	2.84	11.01	2.88	11.09
$Ag_2(SH)_3^-$	2.06	21.25	2.10	21.40
$Ag_3(SH)_4^-$	1.86	31.28	1.92	31.50
$Ag_4(SH)_5^-$	1.76	41.21	1.81	41.52
$Ag_5(SH)_6^-$	1.77	51.16	1.71	51.44
$Ag(SCH_3)_2^-$	2.84	11.15	2.89	11.22
$Ag_2(SCH_3)_3^-$	2.05	21.51	2.10	21.66
$Ag_3(SCH_3)_4^-$	1.90	31.72	1.96	31.96
$Ag_4(SCH_3)_5^-$	1.81	41.83	1.85	42.15
$Ag_5(SCH_3)_6^-$	1.82	51.96	1.89	52.37
$Ag(SPh)_2^-$	2.61	10.18	2.61	10.13
$Ag_2(SPh)_3^-$	1.82	19.57	1.88	19.53
$Ag_3(SPh)_4^-$	1.73	28.86	1.83	28.87
$Ag_4(SPh)_5^-$	1.67	38.02	1.75	37.99
	MUE	0.056	MAD	0.061

comparison with overall binding energy calculated as $E_{overall} = E[M_{13}(M_2(SR)_3)_6^-] - E[M_{13}^{+5}] - 6E[M_2(SR)_3^-]$ and average binding energy calculated as $E_{average} = E_{overall}/6$.

RESULTS AND DISCUSSION

We performed calculations on cyclic methylthiolate gold clusters (Figure 1) and their anionic chain analogs. The values we calculated for E_{inc} and E_{av} shown in Table 1 are in agreement with Häkkinen, Grönbeck, and co-workers.[6,8] Our cyclic clusters are also in agreement with experimentally known gold structures found by Bau,[2] Simpson et al.,[9] LeBlanc et al.,[10] and Wiseman et al.[11] with sulfur−gold−sulfur bond angles of approximately 180 degrees, and gold−sulfur bond lengths of approximately 2.3 Å. The DFT calculations of the cyclic clusters showed that the dimers have BP86 monomer fragmentation energies of 1.07 eV for the cis configuration and 1.09 eV for the trans configuration. In comparison, the PBE monomer fragmentation energies of the dimers are 1.17 eV for the cis configuration and 1.18 eV for the trans configuration. At the TPSS/TZP level of theory, these fragmentation energies are predicted to be 1.11 and 1.13 eV, respectively. These systems also have average binding energies of 0.54 and 0.55 eV for BP86 and 0.58 and 0.59 eV for PBE. The trimer is much higher in both monomer fragmentation and average binding energies than the dimers. The monomer fragmentation energy is 4.00 eV for BP86 and 4.07 eV for PBE, and average binding energy is 1.69 and 1.75 eV for BP86 and PBE, respectively. The monomer fragmentation energy at the TPSS level of theory is 4.06 eV, so both BP86 and PBE are in good agreement with this functional. As shown in Table 1, the cyclic clusters converge from four to six metal atoms with monomer energies about 1.90 eV for BP86 and about 2.00 eV for PBE, and average binding energies of 1.92 eV for BP86 and about 2.00 eV for PBE. Convergence is achieved when the incremental binding energies do not vary significantly from those of the next smaller sized cluster. Our values are in good agreement with data from Häkkinen.[6]

Incremental energies for both the cyclic clusters and the anionic chains converge after four metals. The cyclic clusters are less stable than the anionic chains. For the cyclic clusters the incremental binding energies converge at 1.92 and 1.97 eV (Table 2) compared to the anionic chains that converge at 2.01 and 2.10 eV with the BP86 and PBE functionals, respectively.

Since both gold and silver nanoparticles are of interest experimentally, we examined binding energies of both gold and silver anionic clusters (Figure 2). The two types of metal clusters have substantially different incremental energies. As seen in Table 2, the gold clusters have higher energy than the silver clusters. The mean unsigned error (MUE) and mean absolute deviation (MAD) between gold and silver clusters are the same at 0.29 eV, meaning that the gold clusters always have higher binding energies than the silver clusters. Thus, the gold thiolate chains are predicted to be more stable than the silver thiolate chains. A similar trend was observed for cyclic clusters.[8]

We also looked at the effect of different residue groups attached to the sulfur. With the attachment of hydrogen we see incremental binding energies of 3.24 eV for the $Au(SH)_2^-$ and 2.84 eV for $Ag(SH)_2^-$ at the BP86/TZP level of theory. As the cluster size increases we see a decrease in incremental energy, from approximately 3.24 and 2.84 eV for systems with one metal atom to 2.00 and 1.77 eV for $Au_5(SH)_6^-$ and $Ag_5(SH)_6^-$, respectively. The incremental fragmentation energy appears to converge approximately for clusters with four to five metal atoms.

Changing residue groups to methyl does not change the energies by a significant amount: $Au(SCH_3)_2^-$ and $Ag(SCH_3)_2^-$ have incremental fragmentation energies of 3.22 and 2.84 eV at the BP86/TZP level of theory. The same trend for increasing cluster size holds true: $Au_5(SCH_3)_6^-$ and $Ag_5(SCH_3)_6^-$ both have lower energies than their smaller counterparts with E_{inc} energies of 2.01 and 1.82 eV. Again, the incremental fragmentation energies converge at four to five metal atom clusters.

The change to phenyl as the residue group shows different results than observed with the other two residue groups. The smallest phenyl clusters have E_{inc} energies of 2.99 eV for gold and 2.61 eV for silver. The E_{inc} energies also decrease with the growth of the clusters. $Au_4(SPh)_5^-$ has incremental energies of 1.83 eV for BP86 and 1.99 eV for PBE and $Ag_4(SPh)_5^-$ has energies

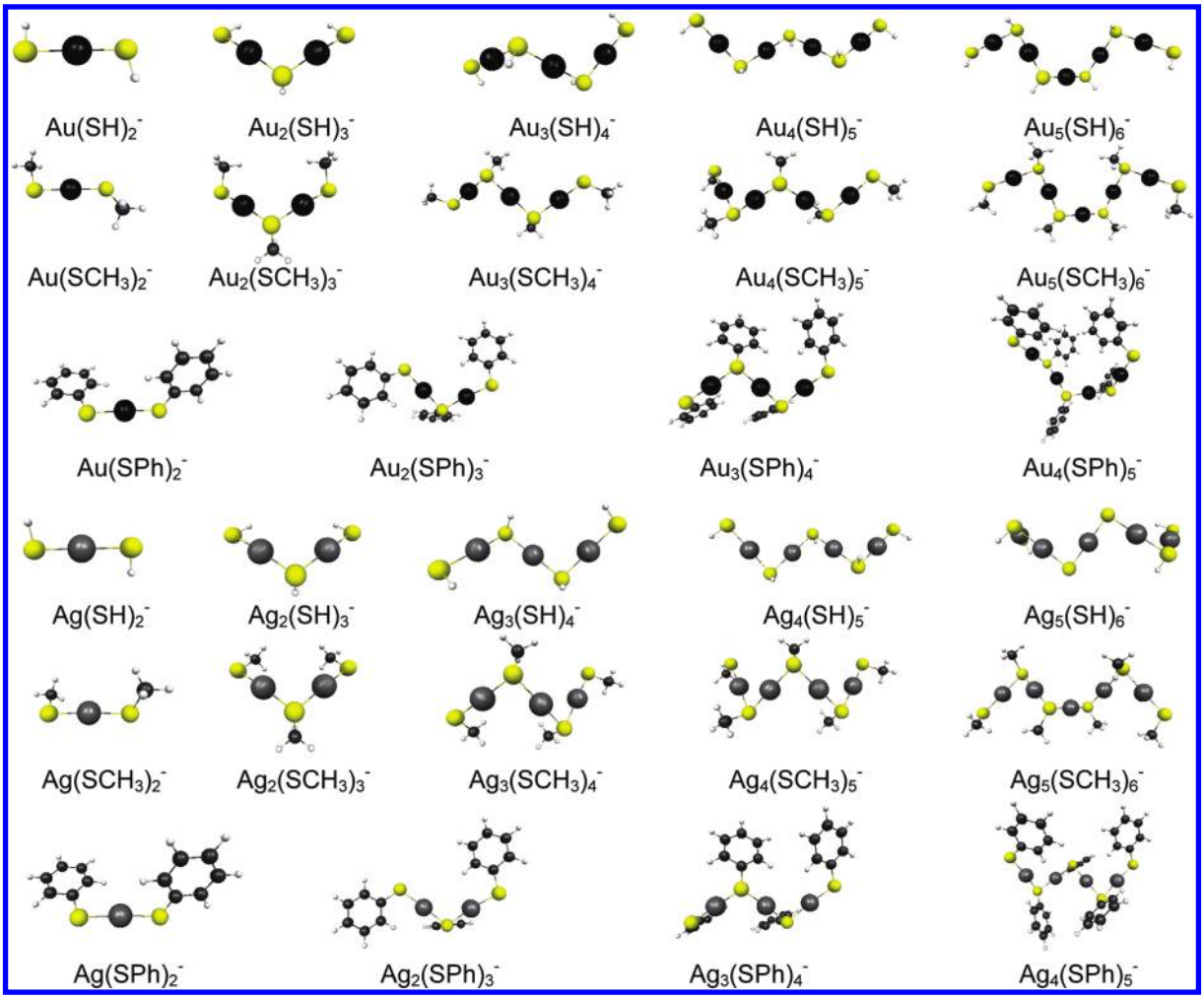

Figure 2. Optimized anionic chain structures for $M_x(SR)_y^-$ (M = Au and Ag; R = H, CH_3, and Ph; $x = 1-5$; $y = 2-6$). Key: Au: black; Ag: silver; S: yellow; C: gray; H: white.

of 1.67 eV for BP86 and 1.75 eV for PBE. We expect that the E_{inc} values for this system also converge after four metal atoms, which suggests that additional AuSPh and AgSPh units will bind with E_{inc} values of approximately 1.83 and 1.99 eV for gold with BP86 and PBE, respectively, and 1.67 and 1.75 eV for silver with BP86 and PBE. This suggests that the energies of formation are significantly different for aliphatic and aromatic ligands. As the clusters grow in size, their incremental energies decrease, but their total energy increases in a linear fashion. The increase in total energy is expected because larger molecules have a greater overall binding energy.

On the basis of the DFT calculations that we have performed on the gold and silver thiolate anionic chain clusters, the BP86 functional generally resulted in a slightly lower energy than the PBE functional, with a MUE of 0.056 eV and a MAD of 0.061 eV. The slight difference in values comes from the reversal of the trend on a few of the phenylthiolate clusters. Energies can be specifically compared in Table 2. TPSS incremental binding energies for $Au(SCH_3)_2^-$ and $Au_2(SCH_3)^-$ are predicted to be 3.22 and 2.31 eV, respectively, which are in very good agreement with the BP86 results and only differ slightly from the PBE values.

BP86 calculations with a quadruple-ζ basis set are employed to determine the effects of larger basis sets. Fragmentation energies calculated with the TZP basis set are generally lower than energies calculated with the QZ4P basis set. The MUE between the TZP and QZ4P is 0.022, and the MAD is 0.029. The difference in MUE and MAD values comes from some of the small methylthiolate silver clusters that have lower energy with QZ4P than TZP as seen in Table 3.

For both of the functionals and basis sets compared in this work, differences between various levels of theory are less than the differences obtained by changing metal atoms or residue groups. The change in the functionals account for about 3% of the total E_{inc} and the basis sets are about 1% of the total E_{inc}, which means that they account for only a small fraction of the total. In seeing this comparison and with the thought of cost and run time in mind, a calculation using either functional will give a reasonable value with a MUE again of 0.022 and 0.056 and a MAD of 0.029 and 0.061 for the basis set and functionals, respectively. For our calculations the smaller basis set yields answers within about 0.02 to 0.03 eV of those of the quadruple basis set, and this level of accuracy is sufficient for this work.

In addition to examining anionic chains, we have also studied the binding energies of the $[M_2(SH)_3]^-$ units to icosahedral metal cores to form $M_{25}(SH)_{18}^-$ nanoparticles. We investigate the pure gold, pure silver, and mixed systems that were previously studied in ref 31. The 13-atom core metal nanoclusters of gold and silver show the same trends that the other clusters studied

Table 3. Basis Set Effects on the Binding Energies of Gold- and Silver-Thiolate Anionic Chains

	BP86/QZ4P	
	E_{inc} (eV)	E_{total} (eV)
$Au(SH)_2^-$	3.26	13.38
$Au_2(SH)_3^-$	2.45	25.94
$Au_3(SH)_4^-$	2.19	38.25
$Au(SCH_3)_2^-$	3.24	13.67
$Au_2(SCH_3)_3^-$	2.36	26.44
$Au_3(SCH_3)_4^-$	2.17	39.03
$Au(SPh)_2^-$	3.08	12.67
$Au_2(SPh)_3^-$	2.17	24.42
$Au_3(SPh)_4^-$	2.02	36.03
$Ag(SH)_2^-$	2.84	11.03
$Ag_2(SH)_3^-$	2.07	21.29
$Ag_3(SH)_4^-$	1.85	31.33
$Ag(SCH_3)_2^-$	2.82	11.18
$Ag_2(SCH_3)_3^-$	2.03	21.56
$Ag_3(SCH_3)_4^-$	1.88	31.79
$Ag(SPh)_2^-$	2.61	10.24
$Ag_2(SPh)_3^-$	1.83	19.69
$Ag_3(SPh)_4^-$	1.77	29.08
MUE	0.022	
MAD	0.029	

Table 4. BP86/TZP Overall and Average Binding Energies of $M_2(SH)_3^-$ to the Icosahedral Core of $M_{25}(SH)_{18}^-$ Nanoclusters

cluster sizes	$E_{overall}$ (eV)	$E_{average}$ (eV)
$Ag_{13}(Au_2(SH)_3)_6^-$	63.88	10.65
$Au_{13}(Ag_2(SH)_3)_6^-$	71.33	11.89
$Ag_{13}(Ag_2(SH)_3)_6^-$	65.15	10.86
$Au_{13}(Au_2(SH)_3)_6^-$	69.97	11.66

show. The gold core binds stronger to the ligands than the silver core; however, both cores bind stronger to the silver ligands than the gold ligands, as seen in Table 4. The silver cores have overall binding energies of 63.88 eV for the gold motifs and 65.15 eV for the silver motifs and the corresponding gold cores have overall binding energies of 69.97 eV for the gold motifs and 71.33 eV for the silver motifs. The average binding energies show the same trend: the silver core with the gold motifs has an average binding energy of 10.65 eV and with the silver motifs it has an average energy of 10.86 eV. The gold core with gold motifs has an average energy of 11.66 eV, and with the silver motifs it has an average energy of 11.89 eV. This could be explained in two ways: that the silver ligands are unstable by themselves in solution or that the cores are very strongly bound to the silver ligands.

CONCLUSIONS

In this body of work, we have shown that the incremental binding energies of cyclic clusters and anionic chains converge after four metal atoms, and that the cyclic clusters are less stable than their anionic analogs. Our cyclic cluster models are in agreement with experimentally known structures and calculations.

We have also shown that there is no significant difference between the BP86 and PBE functionals as well as between the triple-ζ and quadruple-ζ basis sets. Both contribute very little to the total monomer fragmentation energy; the choice of functional affects the energy by about three percent and the basis set yields differences of only about one percent. A larger factor for energy change comes from the changing of residue groups. The hydrogen and methyl groups showed similar energies, whereas the phenyl group showed lower binding energies.

The icosahedral core metal nanoparticles show the same trends as the smaller clusters. The gold cores have higher overall binding and average binding energies than the silver cores. However, the silver thiolate motifs have higher energies in both categories than the gold thiolate motifs.

AUTHOR INFORMATION

Corresponding Author
*E-mail: cmaikens@ksu.edu.

ACKNOWLEDGMENT

The authors thank the Air Force Office of Scientific Research (AFOSR) for funding under Grant FA9550-09-1-0451. C.M.A. is a 2011 Alfred P. Sloan Research Scholar.

REFERENCES

(1) Shaw, C. F., III. *Chem. Rev.* **1999**, *99*, 2589–2600.
(2) Bau, R. *J. Am. Chem. Soc.* **1998**, *120*, 9380–9381.
(3) Daniel, M. C.; Astruc, D. *Chem. Rev.* **2004**, *104*, 293–346.
(4) Kim, K.; Lee, Y. M.; Lee, H. B.; Shin, K. S. *Biosens. Bioelectron.* **2009**, *24*, 3615–3621.
(5) Howell, J. A. S. *Polyhedron* **2006**, *25*, 2993–3005.
(6) Grönbeck, H.; Walter, M.; Häkkinen, H. *J. Am. Chem. Soc.* **2006**, *128*, 10268–10275.
(7) Shao, N.; Pei, Y.; Gao, Y.; Zeng, X. C. *J. Phys. Chem. A* **2009**, *113*, 629–632.
(8) Kacprzak, K. A.; Lopez-Acevedo, O.; Häkkinen, H.; Grönbeck, H. *J. Phys. Chem. C* **2010**, *114*, 13571–13576.
(9) Simpson, C. A.; Farrow, C. L.; Tian, P.; Billinge, S. J. L.; Huffman, B. J.; Harkenss, K. M.; Cliffel, D. E. *Inorg. Chem.* **2010**, *49*, 10858–10866.
(10) LeBlanc, D. J.; Lock, C. J. L. *Acta Cryst. C* **1997**, *53*, 1765–1768.
(11) Wiseman, M. R.; Marsh, P. A.; Bishop, P. T.; Brisdon, B. J.; Mahon, M. F. *J. Am. Chem. Soc.* **2000**, *122*, 12598–12599.
(12) Ahmed, L. S.; Dilworth, J. R.; Miller, J. R.; Wheatley, N. *Inorg. Chim. Acta* **1998**, *278*, 229–231.
(13) Dance, I. G. *Inorg. Chim. Acta* **1977**, *25*, L17–L18.
(14) Dance, I. G.; Fitzpatrick, L. J.; Rae, A. D.; Scudder, M. L. *Inorg. Chem.* **1983**, *22*, 3785–3788.
(15) Dance, I. G.; Fitzpatrick, L. J.; Craig, D. C.; Scudder, M. L. *Inorg. Chem.* **1989**, *28*, 1853–1861.
(16) Dance, I. G.; Fisher, K. J.; Herath Banda, R. M.; Scudder, M. L. *Inorg. Chem.* **1991**, *30*, 183–187.
(17) Lopez-Acevedo, O.; Tsunoyama, H.; Tsukuda, T.; Häkkinen, H.; Aikens, C. M. *J. Am. Chem. Soc.* **2010**, *132*, 8210–8218.
(18) Qian, H.; Eckenhoff, W. T.; Zhu, Y.; Pintauer, T.; Jin, R. *J. Am. Chem. Soc.* **2010**, *132*, 8280–8281.

(19) Jadzinsky, P. D.; Calero, G.; Ackerson, C. J.; Bushnell, D. A.; Kornberg, R. D. *Science* **2007**, *318*, 430–433.
(20) Heaven, M. W.; Dass, A.; White, P. S.; Holt, K. M.; Murray, R. W. *J. Am. Chem. Soc.* **2008**, *130*, 3754–3755.
(21) Zhu, M.; Aikens, C. M.; Hollander, F. J.; Schatz, G. C.; Jin, R. *J. Am. Chem. Soc.* **2008**, *130*, 5883–5885.
(22) Akola, J.; Walter, M.; Whetten, R. L.; Häkkinen, H.; Grönbeck, H. *J. Am. Chem. Soc.* **2008**, *130*, 3756–3757.
(23) Lopez-Acevedo, O.; Akola, J.; Whetten, R. L.; Grönbeck, H.; Häkkinen, H. *J. Phys. Chem. C* **2009**, *113*, 5035–5038.
(24) Grönbeck, H.; Häkkinen, H.; Whetten, R. L. *J. Phys. Chem. C* **2008**, *112*, 15940–15942.
(25) Maksymovych, P.; Sorescu, D. C.; Yates, J. T., Jr. *Phys. Rev. Lett.* **2006**, *97*, 146103[4 pages].
(26) Cossaro, A.; Mazzarello, R.; Rousseau, R.; Casalis, L.; Verdini, A.; Kohlmeyer, A.; Floreano, L.; Scandolo, S.; Morgante, A.; Klein, M. L. *Science* **2008**, *321*, 943–946.
(27) Jiang, D.-e.; Da, S. *Phys. Chem. Chem. Phys.* **2009**, *11*, 8601–8605.
(28) Pei, Y.; Gao, Y.; Shao, N.; Zeng, X. C. *J. Am. Chem. Soc.* **2009**, *131*, 13619–13621.
(29) Jiang, D.-e.; Chen, W.; Whetten, R. L.; Chen, Z. *J. Phys. Chem. C* **2009**, *113*, 16983–16987.
(30) Song, Y.; Harper, A. S.; Murray, R. W. *Langmuir* **2005**, *21*, 5492–5500.
(31) Aikens, C. M. *J. Phys. Chem. C* **2008**, *112*, 19797–19800.
(32) Perdew, J. P. *Phys. Rev. B* **1986**, *33*, 8822–8824.
(33) Becke, A. D. *Phys. Rev. A* **1988**, *38*, 3098–3100.
(34) Perdew, J. P.; Burke, K. B.; Ernzerhof, M. *Phys. Rev. Lett.* **1996**, *77*, 3865–3868.
(35) Tao, J.; Perdew, J. P.; Staroverov, V. N.; Scuseria, G. E. *Phys. Rev. Lett.* **2003**, *91*, 146401[4 pages].
(36) te Velde, G.; Bickelhaupt, F. M.; Baerends, E. J.; Fonseca Guerra, C.; van Gisbergen, S. J. A.; Snijders, J. G.; Ziegler, T. *J. Comput. Chem.* **2001**, *22*, 931–967.
(37) van Lenthe, E.; Ehlers, A. E.; Baerends, E. J. *J. Chem. Phys.* **1999**, *110*, 8943[11 pages].